FREQUENCY DEPENDENCE IN DYNAMICAL GAP GENERATION IN GRAPHENE*

M.E. Carrington

Department of Physics, Brandon University, Manitoba, R7A 6A9 Canada

(Received February 16, 2017)

We study frequency dependencies in the renormalization of the fermion Green function for the π-band electrons in graphene and their influence on dynamical gap generation at sufficiently strong interaction. We use the effective QED-like description for the low-energy excitations within the Dirac-cone region and self consistently solve the fermion Dyson–Schwinger equation using different approximations for the photon propagator and the vertex function. We specifically study frequency-dependent Lindhard screening and retardation effects.

DOI:10.5506/APhysPolBSupp.10.519

1. Introduction

Graphene is a 2-dimensional crystal of carbon atoms which exhibits interesting quantum effects and some unique electronic properties. We consider the simplest form, mono-layer graphene at half filling (zero chemical potential). The carbon atoms are arranged in a 2-dimensional hexagonal lattice and the low-energy dynamics is described by a continuum quantum field theory in which the electronic quasi-particles have a linear Dirac-like dispersion relation of the form of $E = \pm v_{\rm F} p$, where $v_{\rm F} \sim c/300$ is the velocity of a massless electron in graphene. The effective coupling is $\alpha = e^2/(4\pi\epsilon\hbar v_{\rm F})$, where $\epsilon \leq 1$ is related to the physical properties of the graphene sheet. Since $v_{\rm F} \sim c/300$, the system is strongly coupled and non-perturbative methods must be used. The maximum possible effective coupling is obtained with the vacuum value $\epsilon = 1$ and is about $\alpha_{\rm max} = 2.2$.

An important question is whether or not the quasi-particle interactions are strong enough to produce a gap and cause the system to undergo a phase transition to an insulating state. Measurements of the conductivity of

* Presented at the "Critical Point and Onset of Deconfinement" Conference, Wrocław, Poland, May 30–June 4, 2016.

suspended graphene have shown that the insulating state is not physically realizable [1]. However, the experimental observation of fairly strong Fermi velocity renormalization effects indicate that it might be possible to induce a transition via magnetic catalysis [2].

We use the effective QED-like description for the low-energy excitations within the Dirac-cone region, which does not take into account physical screening effects. Within this description however, we go beyond the non-relativistic Coulomb interaction and systematically investigate the various frequency dependencies including retardation effects.

The Euclidean action of the low-energy effective theory is given by

$$\begin{aligned} S &= \int \mathrm{d}^3x \sum_a \bar{\psi}_a \left(i\partial_\mu - eA_\mu\right) M_{\mu\nu}\gamma_\nu \psi_a \\ &\quad -\frac{\epsilon}{4e^2}\int \mathrm{d}^3x F_{\mu\nu}\frac{1}{2\sqrt{-\partial^2}}F_{\mu\nu} + \text{gauge fixing}\,, \end{aligned}$$

where the Greek indices take values $\in \{0,1,2\}$. Four-component Dirac spinors represent quasi-particle excitations on both sub-lattices, with momenta close to either of the two Dirac points. The true spin of the electrons formally appears as an additional flavour quantum number, and we take $N_\mathrm{f} = 2$ for monolayer graphene. The three 4-dimensional γ-matrices form a reducible representation of the Clifford algebra $\{\gamma_\mu, \gamma_\nu\} = 2\delta_{\mu\nu}$ in 2+1 dimensions. M is a diagonal 3×3 matrix defined $M = (1, v_\mathrm{F}, v_\mathrm{F})_\mathrm{diag}$. Lorentz invariance is explicitly broken by the presence of this matrix with $v_\mathrm{F} \neq 1$. The gauge field action is non-local because the photon which mediates the interactions between the electrons propagates out of the graphene plane, in the bulk of the 3+1 dimensional space-time [2,3].

We use self-consistently calculated fermion dressing functions but a one-loop photon polarization tensor calculated with bare lines. The vanishing of the density of states at the Dirac points makes this a reasonable approximation. We include vertex corrections (using an Ansatz which is constructed to preserve gauge invariance). A complete description of how our calculation is related to previous non-relativistic approaches can be found in [4].

2. Notation

We use the notation $Q_\mu = (q_0, \vec{q})$, $Q^2 = q_0^2 + q^2$, $\int \mathrm{d}Q = \int \frac{\mathrm{d}q_0\,\mathrm{d}^2q}{(2\pi)^3}$ and similarly for the momenta P and $K = P - Q$. The fermion propagator contains three dressing functions which we call $Z(p_0, \vec{p})$, $A(p_0, \vec{p})$ and $\Delta(p_0, \vec{p})$. Defining the diagonal 3×3 matrix $\boldsymbol{A}(p_0, \vec{p}) = (Z(p_0, \vec{p}), A(p_0, \vec{p}),$

$A(p_0,\vec{p}))_{\rm diag}$, the inverse fermion propagator has the form of

$$\begin{aligned} S^{-1}(P) &= S_0^{-1}(P)+\Sigma(P) = -i\gamma_\mu \boldsymbol{A}_{\mu\nu}(p_0,\vec{p})M_{\nu\tau}P_\tau + \Delta(p_0,\vec{p})\,, \\ \Sigma(P) &= e^2\int {\rm d}K G_{\mu\nu}(q_0,\vec{q})M_{\mu\tau}\gamma_\tau S\big(k_0,\vec{k}\,\big)\Gamma_\nu\,. \end{aligned} \tag{1}$$

In Landau gauge, the photon propagator is

$$\begin{aligned} G_{\mu\nu} &= \frac{P^1_{\mu\nu}}{G_{\rm T}(q_0,\vec{q})}+P^3_{\mu\nu}\left(\frac{1}{G_{\rm L}(q_0,\vec{q})}-\frac{1}{G_{\rm T}(q_0,\vec{q})}\right), \\ G_{\rm T}(q_0,\vec{q}) &= 2\sqrt{Q^2}+\alpha(q_0,\vec{q})\,, \qquad G_{\rm L}(q_0,\vec{q})=2\sqrt{Q^2}+\alpha(q_0,\vec{q})+\gamma(q_0,\vec{q})\,, \end{aligned} \tag{2}$$

where we have used

$$\begin{aligned} P^1_{\mu\nu} &= \delta_{\mu\nu}-\frac{Q_\mu Q_\nu}{Q^2}\,, \qquad P^3_{\mu\nu}=\frac{Q^2}{q^2}\left(\delta_{0\mu}-\frac{q_0Q_\mu}{Q^2}\right)\left(\delta_{0\nu}-\frac{q_0Q_\nu}{Q^2}\right), \\ \alpha(q_0,\vec{q}) &= \alpha\pi v_{\rm F}\sqrt{q_0^2+v_{\rm F}^2q^2}\,, \qquad \alpha(q_0,\vec{q})+\gamma(q_0,\vec{q})=\frac{\alpha\pi v_{\rm F}Q^2}{\sqrt{q_0^2+v_{\rm F}^2q^2}}\,. \end{aligned} \tag{3}$$

In order to preserve the gauge invariance, we define a non-covariant extension of the Ball–Chiu vertex [5]

$$\begin{aligned} \Gamma_\mu =& \frac{1}{2}M_{\mu\tau}\left(\boldsymbol{A}_{\tau\nu}(p_0,\vec{p})+\boldsymbol{A}_{\tau\nu}\big(k_0,\vec{k}\,\big)\right)\gamma_\nu \\ &+\left[\frac{1}{2}(P_\sigma+K_\sigma)M_{\sigma\tau}\left(\boldsymbol{A}_{\tau\nu}(p_0,\vec{p})-\boldsymbol{A}_{\tau\nu}\big(k_0,\vec{k}\,\big)\right)\gamma_\nu+i\left(\Delta(p_0,\vec{p})-\Delta\big(k_0,\vec{k}\,\big)\right)\right] \\ &\times\frac{(P_\mu+K_\mu)}{P^2-K^2} \end{aligned} \tag{4}$$

which satisfies the Ward identity $-iQ_\mu\Gamma_\mu = S^{-1}(p_0,\vec{p})-S^{-1}(k_0,\vec{k}\,)$. Using this vertex in (1) is what we call the BALL–CHIU calculation. Simpler expressions are obtained if we use only the first term in the Ball–Chiu vertex. We call this the SHORT calculation.

A further approximation is to expand simultaneously in $\{v_{\rm F}, q_0/q\}\sim\delta$. The expansion in q_0/q is motivated by the fact that the photons that mediate the Coulomb interaction move much more quickly than the electrons, and, therefore, the interaction can be taken to be almost instantaneous. In this approximation, the transverse modes drop out and the longitudinal part of the propagator is replaced with the Coulomb propagator $G_{00}^{-1} = 2q+\Pi_{00}(q_0,q)$. We refer to this as the COULOMB calculation. It was done previously in Ref. [6]. We will also compare it with an early calculation in

the literature [7] that used much more restrictive assumptions: bare vertices, no magnetic modes, frequency independent fermion dressing functions, and the instantaneous approximation.

The integral equations that determine the dressing functions in the SHORT calculation are

$$Z_p = 1 - \frac{2\alpha\pi v_{\rm F}}{p_0} \int {\rm d}K \frac{k_0 q^2 Z_k Z_s}{Q^2\, G_{\rm L} S_k}\,, \tag{5}$$

$$A_p = 1 + \frac{2\alpha\pi v_{\rm F}}{p^2} \int {\rm d}K\, \frac{q^2 A_k Z_s \vec{k}\cdot\vec{p} + k_0 q_0 Z_k (Z_s + A_s)\vec{p}\cdot\vec{q}}{Q^2\, G_{\rm L} S_k}\,, \tag{6}$$

$$D_p = 2\alpha\pi v_{\rm F} \int {\rm d}K \frac{q^2 \Delta_k Z_s}{Q^2\, G_{\rm L} S_k}\,, \tag{7}$$

where we have defined $Z_p = Z(p_0, \vec{p})$, $Z_s = Z_p + Z_k$, $Z_d = Z_p - Z_k$, *etc.* and $G_{\rm L} = G_{\rm L}(q_0, \vec{q})$ and $S_k = k_0^2 Z_k^2 + k^2 A_k^2 v_{\rm F}^2 + \Delta_k^2$. The analogous expressions for the COULOMB and BALL–CHIU calculations are given in [4].

3. Results

To do the momentum integrals, we introduce an ultra-violet cut-off Λ and use a logarithmic scale. We define dimensionless variables $\hat{k}_0 = k_0/\Lambda$, $\hat{p}_0 = p_0/\Lambda$, $\hat{k} = k/\Lambda$, $\hat{p} = p/\Lambda$ and $\hat{\Delta} = \Delta/\Lambda$. The hatted frequency and momentum variables range from zero to one, and all hats are suppressed from this point. In Fig. 1 (top), we show the gap *versus* α for four different calculations. We fit this data and the resulting function is extrapolated to obtain the value of the critical coupling for which the gap goes to zero. The critical coupling can also be obtained from a bifurcation analysis. The results are shown in Table I. The BALL–CHIU and SHORT calculations agree well, while the COULOMB calculation gives a slightly smaller critical coupling. The frequency-independent calculation gives a significantly larger result than the calculations which take into account the frequency dependence of the dressing functions. In all cases, the result is bigger than the largest physically realizable coupling $\alpha_{\rm max} \sim 2.2$.

In Fig. 1 (bottom), we show the renormalized Fermi velocity, which is defined as $A(p_0, p)/Z(p_0, p)$, as a function of momentum. The increase in the Fermi velocity at small coupling which is observed experimentally is clearly seen.

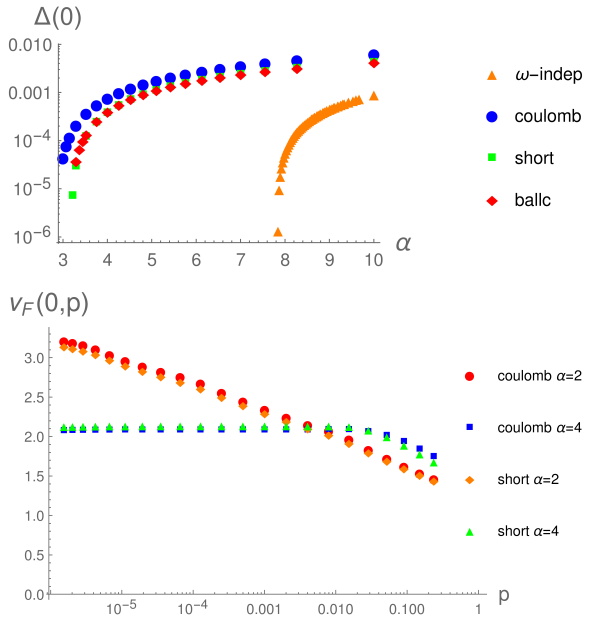

Fig. 1. Numerical results for the gap and renormalized fermion velocity. Top: $\Delta(0)$ *versus* α; Bottom: $A(0,p)/Z(0,p)$ *versus* p.

TABLE I

Results for critical values of the coupling α.

Calculation	α_c	Bifurcation range
ω-independent	8.967	
COULOMB	2.906	2.900–2.899
SHORT	3.190	3.190–3.191
BALL-CHIU	3.178	

4. Conclusions

We have done a calculation of the dynamically generated gap in monolayer suspended graphene, starting from a low-energy effective field theory. Our calculations contain three effects that have not previously been included: vertex corrections, magnetic effects and full frequency dependence in dressing functions and loop integrals. The precise numerical values of the critical couplings that we obtain are not meant to be realistic, since they will clearly be changed (in a predictable manner) by short distance screening effects which we have not included. However, attempts to include

realistic interactions on the honeycomb lattice have usually been done in static approximations or dynamical mean field theory [8]. Both approaches work towards the final goal of a calculation that includes both frequency-dependent effects and realistic screening, from complementary directions.

REFERENCES

[1] D.C. Elias *et al.*, *Nature Phys.* **7**, 701 (2011).

[2] E.V. Gorbar, V.P. Gusynin, V.A. Miransky, I.A. Shovkovy, *Phys. Rev. B* **66**, 045108 (2002).

[3] E.C. Marino, *Nucl. Phys. B* **408**, 551 (1993).

[4] M.E. Carrington, C.S. Fischer, L. von Smekal, M.H. Thoma, *Phys. Rev. B* **94**, 125102 (2016).

[5] J.S. Ball, T.W Chiu, *Phys Rev. D* **22**, 2542 (1980).

[6] J.-R. Wang, G.-Z. Liu, *New J. Phys.* **14**, 043036 (2012).

[7] C. Popovici, C.S. Fischer, L. von Smekal, *Phys. Rev. B* **88**, 205429 (2013).

[8] T.O. Wehling *et al.*, *Phys. Rev. Lett.* **106**, 236805 (2011); M.V. Ulybyshev, P.V. Buividovich, M.I. Katsnelson, M.I. Polikarpov, *Phys. Rev. Lett.* **111**, 056801 (2013); D. Smith, L. von Smekal, *Phys. Rev. B* **89**, 195429 (2014).